

# Dynamics and Thermodynamics of Axial Ligation in Metalloporphyrins. 4. Kinetics of Porphyrin Inversion in High-Spin Ferric Complexes

Richard V. Snyder and Gerd N. La Mar\*<sup>1</sup>

Contribution from the Department of Chemistry, University of California, Davis, California 95616. Received September 15, 1975

**Abstract:** The mobility of the high-spin ferric ion relative to the heme plane was investigated for a series of synthetic porphyrin ferric halide complexes. Motion of the metal through the hole (inversion) was induced by two distinct mechanisms. In the presence of excess halide ion, the porphyrins inverted by an associative mechanism. Second-order rate constants for a variety of porphyrin complexes revealed that the rate of inversion increased with decreasing porphyrin basicity, decreasing axial ligand field strength, and increasing solvent dielectric constant. Activation parameters were obtained for four complexes, which indicate that the changes in rates are primarily enthalpy effects. For weak axial ligands inversion was also found to proceed via a dissociative mechanism involving the ionic form of the porphyrin. The rapid rates of inversion obtained in this study reflect a high degree of mobility of high-spin iron relative to the porphyrin plane and suggest that both the Fe(III) and Fe(II) ions could pass readily through the porphyrin hole without converting to the low-spin forms. The possible role of porphyrin deformations in effecting this inversion is discussed.

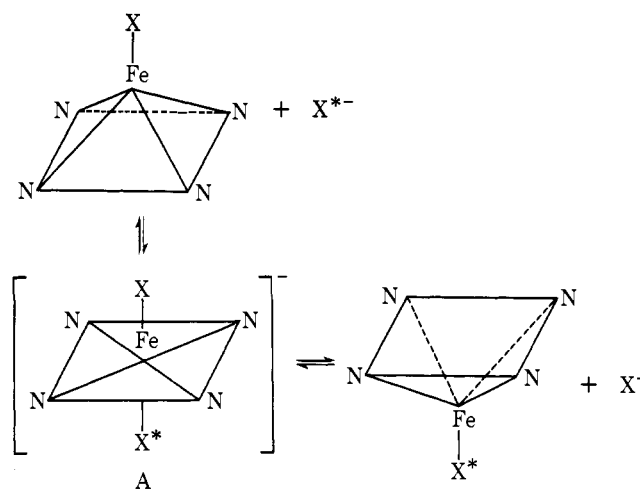
## Introduction

A characteristic property of iron porphyrin complexes is that five-coordinate species are high-spin (HS), with the metal ion displaced some 0.4–0.8 Å above the porphyrin plane.<sup>2,3</sup> It has been postulated that the large ionic radii of HS Fe(III) and Fe(II) preclude the possibility that they can fit into the porphyrin hole, which has a more or less fixed dimension, and hence that there is a significant stabilization of the energy by this out-of-plane displacement.<sup>2,3</sup> Upon addition of a sixth ligand, the metal ion generally converts to the smaller, low-spin (LS) form which easily fits into the porphyrin hole within the porphyrin plane.<sup>4,5</sup>

A similar relationship between coordination number, spin state, and position of the iron relative to the heme plane exists in the heme proteins myoglobin and hemoglobin.<sup>6–8</sup> In the latter tetraheme protein, the cooperativity with respect to oxygenation has been proposed<sup>2a,6,8</sup> to arise from rearrangement of the peptide chain attached to the proximal histidine due to the motion of the iron. Hence the conversion of the HS, out-of-plane iron to LS, in-plane iron has been termed the “trigger” in this model of cooperativity.<sup>8</sup> A basic assumption of this model is that there is a significant barrier to bringing a high-spin iron near the porphyrin plane. However, it has been suggested<sup>9</sup> elsewhere that high-spin iron could have appreciable mobility relative to the heme plane, which would indicate a relatively low barrier towards bringing the HS iron into the heme plane.

The observations<sup>2–5,10–13</sup> that the degree of nonplanarity of the tetrapyrrole skeleton differs widely and that the size of the “hole” varies by about 0.3 Å over a range of metal ions suggest that the porphyrin skeleton can indeed be deformed readily, and thereby accommodate large metal ions close to the heme more easily than suggested by static structural studies.

Since the activation energy for bringing the metal ion into the plane is related to the thermodynamic stabilization energy for the out-of-plane displacement,<sup>14</sup> we have investigated<sup>15,16</sup> the kinetics of porphyrin *inversion* in order to shed light on the mobility of the iron relative to the heme plane. Inversion is the term for the process whereby the HS metal ion moves from one side of the porphyrin plane, through the hole, to the other side. We had earlier demonstrated<sup>15,16</sup> that the pair of *m*-H peaks in the proton NMR spectra of tetraarylporphyriniron(III) halide<sup>17</sup> (R-TPPFEX), as well as the  $\alpha$ -CH<sub>2</sub> doublet of oc-



taethylporphyriniron(III) halide<sup>18</sup> (OEPFeX), can serve as selective probes for the dynamics of inversion. Initially, we considered<sup>15</sup> inversion induced by excess halide ion via A. We are concerned here with the detailed characterization of the kinetics and mechanism for inversion via A and the question as to whether the ferric ion in the activated complex is HS or LS. It will also be shown that inversion can be induced via a dissociative pathway<sup>16</sup> involving the ionic porphyrin PFe<sup>+</sup>. The study of inversion via halogen exchange will also provide kinetic data for axial ligand exchange in five-coordinate porphyrins. Not only is there relatively little known about the axial ligand lability in porphyrins in particular,<sup>19,20</sup> but there is also a paucity of data on mechanisms of ligand exchange in five-coordinated complexes in general.<sup>21</sup> Although halogen exchange may occur via other mechanisms, the NMR method relying on the collapse of the *m*-H or  $\alpha$ -CH<sub>2</sub> peaks is sensitive only to the S<sub>N</sub>2 mechanism<sup>15</sup> depicted in A.

## Experimental Section

The *p*-CH<sub>3</sub>-TPPFeCl, *p*-CH<sub>3</sub>-TPPFeI, and TPPFeCl complexes were prepared by the method of Adler et al.<sup>22</sup> and have been characterized previously.<sup>17,18,23</sup> OEP was a gift from Professor H. H. Inhoffen; the metal was inserted by standard procedure to yield the previously characterized<sup>17,18</sup> OEPFeCl. The iodide complexes were prepared from their respective chlorides by metathesis in methylene chloride with NaI at pH ~3. The TPPFeI complex prepared in this

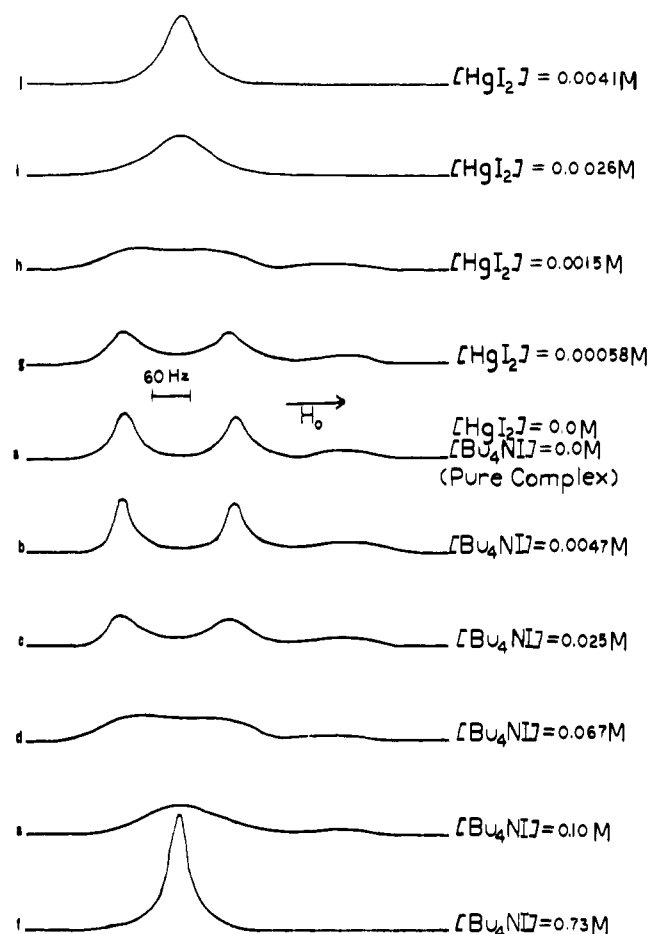


Figure 1. Proton NMR traces of the *m*-H region of *p*-CH<sub>3</sub>-TPPFel in CDCl<sub>3</sub> at 25 °C; a, pure complex; b-f, porphyrin plus increasing amounts of Bu<sub>4</sub>N<sup>+</sup>I<sup>-</sup>; g-j, porphyrin plus increasing amounts of HgI<sub>2</sub>.

manner exhibited a chloride impurity even after successive treatments with NaI; hence only the pure *p*-CH<sub>3</sub>-TPPFel complexes were used. The purity of OEPFeI was confirmed by its proton spectrum and elemental analysis (Anal. Calcd for C<sub>36</sub>H<sub>44</sub>N<sub>4</sub>FeI: C, 60.42; H, 6.20. Found: C, 60.39; H, 6.13).

The tetrafluoroborate salt of tetraphenylporphyrinatoiron(III) was prepared after the method of Reich and Cohen.<sup>24</sup> A benzene solution of  $\mu$ -oxo-bis(tetraphenylporphyrinato)iron(III) was stirred with 2 equiv of aqueous HBF<sub>4</sub> for 2 h and then extracted twice with water. After removing the benzene by water-aspirator vacuum, the product (TPPFeBF<sub>4</sub>) was recrystallized from warm benzene by adding hexane and was characterized by its electronic spectrum ( $\lambda_{\max}$  414, 479, 547, 608 m $\mu$  in CHCl<sub>3</sub>), and its elemental analysis (Anal. Calcd for C<sub>44</sub>H<sub>28</sub>N<sub>4</sub>FeBF<sub>4</sub>: C, 69.9; H, 3.74. Found: C, 70.02; H, 3.91).

The salts tetrabutylammonium triiodomercurate(II) (Bu<sub>4</sub>NHgI<sub>3</sub>) and bis(tetrabutylammonium) tetraiodomercurate(II) ((Bu<sub>4</sub>N)<sub>2</sub>HgI<sub>4</sub>) were prepared by mixing the appropriate molar ratios of Bu<sub>4</sub>N<sup>+</sup>I<sup>-</sup> and HgI<sub>2</sub> in acetone, removing the solvent, and crystallizing the products from acetone using ether. The products gave sharp melting points (126–128 and 134–135 °C, respectively) and the following elemental analyses. Calcd for C<sub>16</sub>H<sub>36</sub>NH<sub>2</sub>I<sub>4</sub>: C, 23.32; H, 4.40. Found: C, 23.47; H, 4.50. Calcd for C<sub>32</sub>H<sub>72</sub>N<sub>2</sub>HgI<sub>4</sub>: C, 32.20; H, 6.08. Found: C, 32.25; H, 6.22.

Tetrabutylammonium tetrafluoroborate was prepared by neutralizing HBF<sub>4</sub> with Bu<sub>4</sub>NOH in an ethanol-water solution. Repeated recrystallizations of the product (Bu<sub>4</sub>NBF<sub>4</sub>) from acetone-ether could not improve the melting range to less than  $\sim$ 10° (142–152 °C) (lit.<sup>25</sup> 162 °C).

Electronic spectra were recorded on a Cary-15 spectrometer. A Jeolco PS-100 FT NMR spectrometer with Digilab NMR-3 computer was used to record the NMR spectra. For variable temperature work, an iron-constantan thermocouple contained in a sample tube was used to calibrate the temperature in the probe to  $\pm$ 1°.

Samples were prepared by weighing the porphyrins and dissolving

them in 0.35 ml of solvent. Other reagents were added as solids (except for HgI<sub>2</sub>), and their concentrations were determined by comparing relative areas of peaks (NCH<sub>2</sub> peak in Bu<sub>4</sub>N<sup>+</sup> salts and methyl peak in *p*-CH<sub>3</sub>TPP or OEP). Aliquots of a saturated chloroform solution of HgI<sub>2</sub> were used to add HgI<sub>2</sub> to NMR samples, evaporating excess solvent with N<sub>2</sub>. The solubility of HgI<sub>2</sub> in chloroform was determined by weighing the residues after evaporation of chloroform from saturated HgI<sub>2</sub> solutions. The value was determined to be  $(2.03 \pm 0.06) \times 10^{-3}$  mol/l.

**Data Treatment.** The rates of exchange of the *m*-H peaks were determined by comparing observed spectra to computer simulated spectra. The simulated spectra were calculated by the program EXCNMR.<sup>26</sup>

Estimates of the rates as input for the program were made using the standard equations for limiting conditions.<sup>27</sup> Observed line widths were corrected for the nonexchange contribution by subtracting out the value of  $\delta_{1/2}$  in the absence of exchange. This was estimated<sup>28</sup> by extrapolating a log  $\delta_{1/2}$  vs.  $1/T$  plot of the *m*-H from low temperature to higher temperatures using the slope of a similar plot of the *p*-CH<sub>3</sub> peak.

**Kinetic Parameters.** The apparent order for a given reagent was determined by plotting ln (rate) vs. the ln (concentration) of that reagent. The slope yielded the order, and was computed using a linear, nonweighted least-squares computer fit.

Activation parameters were determined by assuming the Eyring relation holds and plotting ln ( $k/T$ ) vs.  $1/T$ . The slopes and intercepts were determined by a linear, nonweighted, least-squares fit and were used to calculate  $\Delta H^\ddagger$  and  $\Delta S^\ddagger$ . Values of  $\Delta G^\ddagger$  were calculated at 25 °C from  $\Delta H^\ddagger$  and  $\Delta S^\ddagger$ .

**Uncertainties.** The uncertainty in each value of  $k_2$  represents the standard deviation of the various values of  $k_2$  calculated for a given experiment at several concentrations of added reagent. The uncertainties in the values of  $\Delta H^\ddagger$  and  $\Delta S^\ddagger$  are calculated from the standard errors of the slope and intercept (respectively) from the least-squares computer fit. The uncertainty in  $\Delta G^\ddagger$  was calculated from those in  $\Delta H^\ddagger$  and  $\Delta S^\ddagger$ .

## Results and Discussion

The region of the proton NMR spectrum where the two *m*-H peaks of *p*-CH<sub>3</sub>-TPPFel resonate in CDCl<sub>3</sub> is illustrated in Figure 1. The spectrum is very similar to that of *p*-CH<sub>3</sub>-TPPFel reported<sup>15</sup> earlier, except that all resonances are narrower due to more efficient electron spin relaxation.<sup>23</sup> The effect of adding increasing amounts of excess iodide ion in the form of tetra-*n*-butylammonium iodide (Bu<sub>4</sub>N<sup>+</sup>I<sup>-</sup>) is illustrated in traces a through f of Figure 1. The effect of Bu<sub>4</sub>N<sup>+</sup>I<sup>-</sup> on the pair of *m*-H peaks is qualitatively similar to that reported earlier for the analogous chloride. The iodide complexes generally served as better subjects for the kinetic studies because of the improved spectral resolution.<sup>23</sup> Increasing amounts of Bu<sub>4</sub>N<sup>+</sup>I<sup>-</sup> caused collapse of the pair of *m*-H peaks, with the collapsed peak exhibiting the averaged chemical shift. Hence there appears to be no significant concentration of any long-lived intermediate such as the "activated complex" in A, in contrast to a report of the stable species possessing two coordinated fluorides.<sup>29</sup>

There is, however, at least one important difference between the behavior of *m*-H peak upon addition of the halide salt for the chloride and iodides. The addition of very small amounts, of Bu<sub>4</sub>N<sup>+</sup>I<sup>-</sup> to *p*-CH<sub>3</sub>-TPPFel results first in a small, but clearly observable, decrease in the *m*-H line widths (see traces a and b in Figure 1). A similar effect is observed for OEPFeI. No such narrowing of the peak was observed for the chloride complex. This initial narrowing in a and b of Figure 1 indicates that there is an additional mechanism for porphyrin inversion which occurs in the absence of excess iodide. Such a mechanism would involve dissociative inversion, which is suppressed upon adding small amounts of Bu<sub>4</sub>N<sup>+</sup>I<sup>-</sup> (vide infra).

**Inversion via Associative Halide Exchange.** Initially, we shall be interested in the dynamic process illustrated in traces c-f of Figure 1, for which the rate of collapse of the *m*-H peak increases with Bu<sub>4</sub>N<sup>+</sup>I<sup>-</sup> concentration.

**Table I.** Second Order Rate Constants for Porphyrin "Inversion" via Associative Halide Exchange<sup>a</sup>

Porphyrin complex	Solvent	$k_2^{298, b}$ M <sup>-1</sup> s <sup>-1</sup>
<i>p</i> -CH <sub>3</sub> -TPPFeCl	CDCl <sub>3</sub>	$(5.6 \pm 1.4) \times 10^2$
<i>p</i> -CH <sub>3</sub> -TPPFeI	CDCl <sub>3</sub>	$(5.9 \pm 1.2) \times 10^3$
OEPFeCl	CDCl <sub>3</sub>	$(5.8 \pm 1.2) \times 10$
OEPFeI	CDCl <sub>3</sub>	$(9.0 \pm 1.6) \times 10^2$
<i>p</i> -CH <sub>3</sub> -TPPFeI	CD <sub>2</sub> Cl <sub>2</sub>	$(2.0 \pm 0.4) \times 10^5$
<i>p</i> -CH <sub>3</sub> O-TPPFeCl	CD <sub>2</sub> Cl <sub>2</sub>	$(2.1 \pm 0.4) \times 10^4$
<i>p</i> -CH <sub>3</sub> -TPPFeCl	CD <sub>2</sub> Cl <sub>2</sub>	$(4.2 \pm 0.8) \times 10^4$
<i>p</i> -Cl-TPPFeCl	CD <sub>2</sub> Cl <sub>2</sub>	$(5.6 \pm 0.4) \times 10^4$

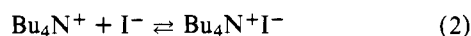
<sup>a</sup> Rate constant as described by eq 1. <sup>b</sup> At 25 °C.

**Rate Law and Mechanism.** This mechanism, depicted in A, should follow the rate law:

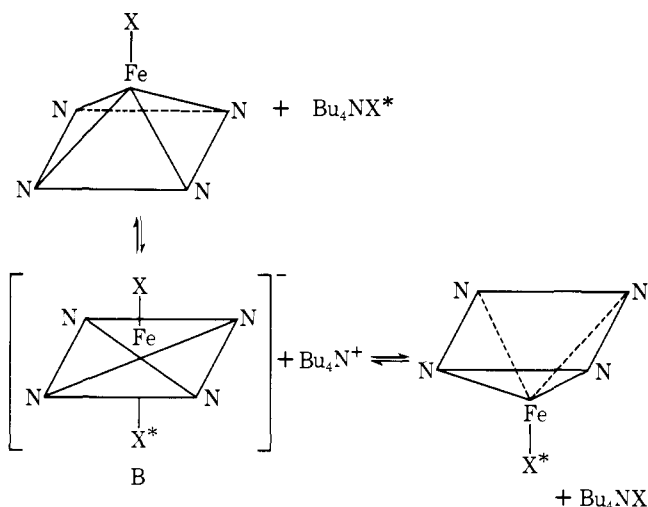
$$\text{rate} = k_2[\text{PFeX}][\text{X}^-] \quad (1)$$

Using line-width data under circumstances where the associative mechanism dominates (i.e., excess Bu<sub>4</sub>N<sup>+</sup>X<sup>-</sup>), the effect on the rate of varying both porphyrin and Bu<sub>4</sub>N<sup>+</sup>X<sup>-</sup> was investigated. As indicated in Figure 2, plots of ln(rate) vs. ln[Bu<sub>4</sub>N<sup>+</sup>X<sup>-</sup>] yield straight lines with slopes of 1.0 ± 0.1 for all porphyrins investigated in CDCl<sub>3</sub>. A similar dependence of the rate on [*p*-CH<sub>3</sub>-TPPFeI] was observed and confirmed the bimolecular nature of the inversion in eq 1.

The well-defined first-order nature with respect to [Bu<sub>4</sub>N<sup>+</sup>X<sup>-</sup>] is somewhat surprising, in that the association constant for the reaction<sup>30</sup>



is estimated to be ~10<sup>4</sup> in CDCl<sub>3</sub>. Hence the primary species at our concentration is the ion-paired form, not the free ions, as required in eq 1. Since we find that the order [Bu<sub>4</sub>N<sup>+</sup>I<sup>-</sup>] does not deviate significantly from unity over a wide range of concentrations, we conclude that the rate with free I<sup>-</sup> as the attacking group does not differ significantly from that with Bu<sub>4</sub>N<sup>+</sup>I<sup>-</sup> as the agent. Thus, the mechanism for A may be more appropriately written as B. The activated complex may also remain ion paired.



A summary of the computed second-order rate constants ( $k_2$ ) (eq 1) is found in Table I; values for CDCl<sub>3</sub> solution are given in the first four rows. The rate data reveal that iodides always invert faster than chlorides.

**Activation Parameters.** The Eyring plots for *p*-CH<sub>3</sub>-TPPFeX and OEPFeX, (X = Cl, I), are reproduced in Figure 3, and the resulting activation parameters are listed in Table II. The difference in rates between chlorides and iodides for

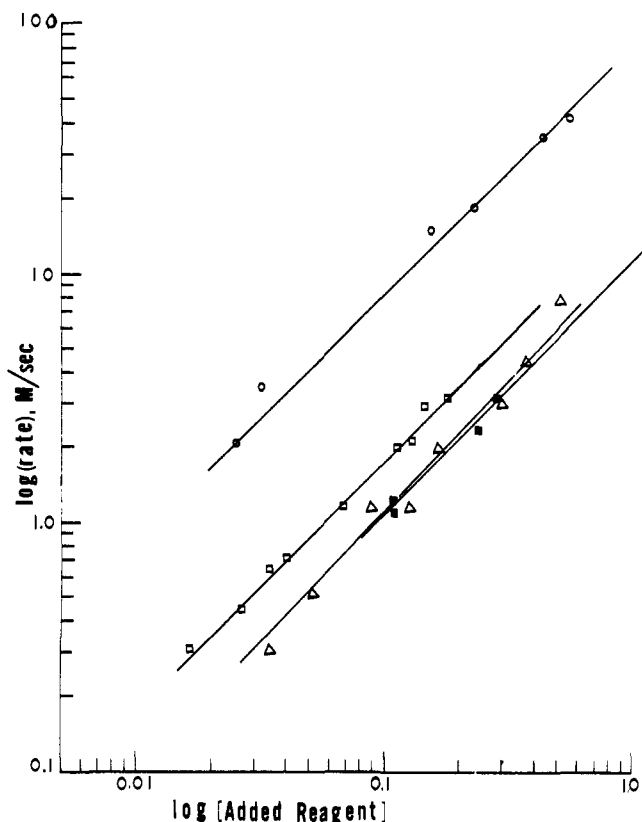


**Figure 2.** Plot of log(rate) vs. log[Bu<sub>4</sub>NX]; □ = [OEPFeI] = 0.020 M and Bu<sub>4</sub>N<sup>+</sup>I<sup>-</sup>; △ = [OEPFeCl] = 0.020 M and Bu<sub>4</sub>N<sup>+</sup>Cl<sup>-</sup>; ■ = [*p*-CH<sub>3</sub>-TPPFeCl] = 0.020 M and Bu<sub>4</sub>N<sup>+</sup>Cl<sup>-</sup>; ○ = [*p*-CH<sub>3</sub>-TPPFeI] = 0.017 M and Bu<sub>4</sub>N<sup>+</sup>I<sup>-</sup>; all in CDCl<sub>3</sub>, △ at 75 °C, others at 25 °C.

**Table II.** Activation Parameter for Porphyrin "Inversion" via Associative Halide Exchange<sup>a</sup>

Porphyrin complex	$\Delta G^\ddagger_{298}$ b,c	$\Delta H^\ddagger$ c	$\Delta S^\ddagger$ d
<i>p</i> -CH <sub>3</sub> -TPPFeCl	14.2 ± 1.2	9.1 ± 0.8	-17 ± 4
<i>p</i> -CH <sub>3</sub> -TPPFeI	12.2 ± 0.6	6.5 ± 0.3	-19 ± 2
OEPFeCl	15.0 ± 1.0	8.8 ± 0.5	-21 ± 2
OEPFeI	13.2 ± 0.4	7.2 ± 0.2	-20 ± 2

<sup>a</sup> For the rate expression described in eq 1. <sup>b</sup> 25 °C. <sup>c</sup> In kcal/mol. <sup>d</sup> In entropy units.

the same porphyrin is seen to originate primarily in smaller  $\Delta H^\ddagger$ 's for the iodides. In the case of fixed halide, the OEP complexes inverted more slowly than *p*-CH<sub>3</sub>-TPP complexes, again due mainly to enthalpy effects (the  $\Delta H^\ddagger$  for *p*-CH<sub>3</sub>-TPPFeCl has a sizable uncertainty,<sup>31</sup> so that the relative value of  $\Delta H^\ddagger$  for OEPFeCl and *p*-CH<sub>3</sub>-TPPFeCl cannot be unambiguously established).

The  $\Delta S^\ddagger$  values are fairly constant, ~-20 ± 3 eu, and their negative sign supports the associative mechanism.

**Solvent Effects.** The rate of inversion of *p*-CH<sub>3</sub>-TPPFeCl in CD<sub>2</sub>Cl<sub>2</sub>, as induced by Bu<sub>4</sub>N<sup>+</sup>X<sup>-</sup>, were found to be first order in [Bu<sub>4</sub>N<sup>+</sup>X<sup>-</sup>], suggesting that eq 1 probably also applies.<sup>32</sup> The second-order rate constants, evaluated on the assumption that eq 1 is valid, are also given in Table I. The faster rates in CD<sub>2</sub>Cl<sub>2</sub> relative to CDCl<sub>3</sub> are probably due to the greater dielectric constant of methylene chloride (9.1) relative to chloroform (4.8), which can be reasonably expected to stabilize the activated complex.

**Porphyrin Substituent Effects.** The data in both CDCl<sub>3</sub> and CD<sub>2</sub>Cl<sub>2</sub> solution indicate that the inversion rates decrease with increased porphyrin basicity. In CD<sub>2</sub>Cl<sub>2</sub>,  $k_2$  increases mono-

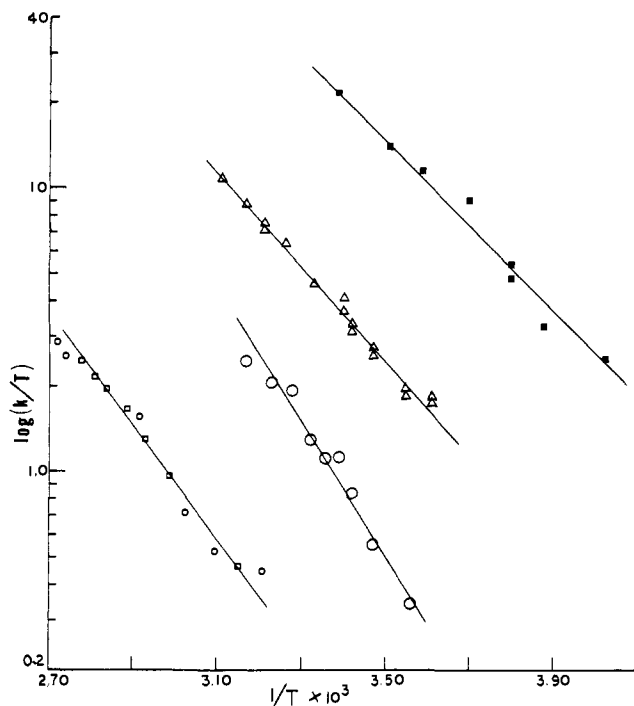
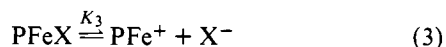


Figure 3. Eyring plots for associative reactions in  $\text{CDCl}_3$ .  $\square$  = OEPFeCl and  $\text{Bu}_4\text{NCl}$ ;  $\circ$  =  $p\text{-CH}_3\text{-TPPFeCl}$  and  $\text{Bu}_4\text{NCl}$ ;  $\blacksquare$  =  $p\text{-CH}_3\text{-TPPFel}$  and  $\text{Bu}_4\text{Nl}$ ;  $\triangle$  = OEPFel and  $\text{Bu}_4\text{Nl}$ .

tonically as R in  $p\text{-R-TPPFeCl}$  is made more electron withdrawing, i.e.,  $p\text{-CH}_3\text{O} < p\text{-CH}_3 < p\text{-Cl}$ .<sup>32</sup> The rate for OEPFeX inversion is considerably slower than for  $p\text{-CH}_3\text{-TPPFeX}$  in  $\text{CDCl}_3$ , since OEP is the most basic porphyrin included in this study. The kinetic parameters in Table II indicate that enthalpy changes dominate the changes in  $k_2$ . This trend is consistent with the proposed mechanism, since increased porphyrin basicity will stabilize the five-coordinate reactant and decrease its affinity for the sixth ligand in the activated complex. A related thermodynamic effect was observed for a series of substituted natural porphyrin derivatives of nickel(II) with nitrogenous bases.<sup>33</sup> Although attempts were made to characterize this inversion mechanism for natural porphyrin derivatives, extensive aggregation even at relatively low concentration prevented clear resolution of the desired  $\alpha\text{-CH}_2$  peaks.

**Inversion via Dissociative Halide Exchange.** As indicated above, even pure  $p\text{-CH}_3\text{-TPPFel}$  (as well as OEPFel) exhibits line broadening at  $25^\circ$ . The inversion rate is highly concentration dependent, increasing slightly faster than  $[p\text{-CH}_3\text{-TPPFel}]$ . At  $25^\circ$  a 0.020 M solution yielded an inversion rate  $\sim 100 \text{ s}^{-1}$ . The effect on the observed rate of inversion of  $p\text{-CH}_3\text{-TPPFel}$  upon addition of  $\text{Bu}_4\text{N}^+\text{I}^-$  is illustrated in Figure 4. For the complex  $p\text{-CH}_3\text{-TPPFelBF}_4$ , which we originally hoped would provide an unliganded "ionic" porphyrin, a single collapsed  $m\text{-H}$  peak was found for the pure complex at  $33^\circ$ , which split into a broadened doublet at  $25^\circ$ ; addition of  $\text{Bu}_4\text{N}^+\text{BF}_4^-$  narrowed the lines.

The observation of inversion in the pure complex for weak axial ligands such as  $\text{I}^-$  and  $\text{BF}_4^-$  (the ability to slow down inversion by addition of  $\text{BF}_4^-$  confirms that the anion is in fact axially coordinated), but not for a stronger ligand such as  $\text{Cl}^-$ , suggests that dissociation of the complex is responsible



Inversion then occurs either in the ionic form or during the recombination (vide infra). Addition of excess  $\text{X}^-$  in the form of  $\text{Bu}_4\text{N}^+\text{X}^-$  would shift the equilibrium in eq 3 to the left,

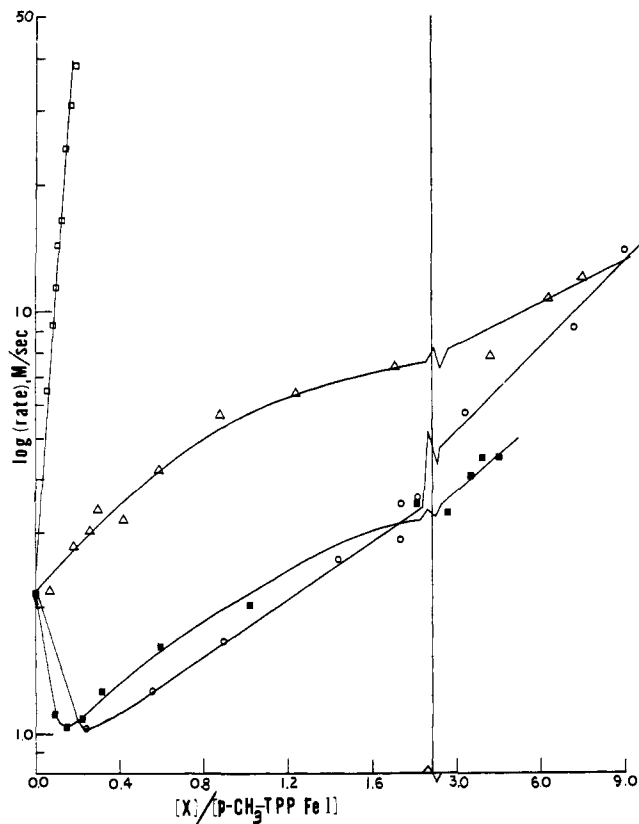
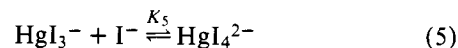
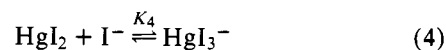


Figure 4. Plot of  $\log(\text{rate})$  vs. concentration of the added reagent (X) divided by porphyrin concentration for  $p\text{-CH}_3\text{-TPPFel}$  in  $\text{CDCl}_3$  at  $25^\circ\text{C}$ .  $\square$  =  $\text{HgI}_2$ ;  $\triangle$  =  $\text{Bu}_4\text{NHgI}_3$ ;  $\circ$  =  $\text{Bu}_4\text{NI}$ ;  $\blacksquare$  =  $(\text{Bu}_4\text{N})_2\text{HgI}_4$ .

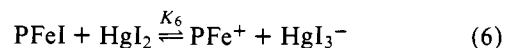
decreasing the rate of inversion by removing the ionic species.

No attempts were made to formulate a rate law for inversion via dissociation, since the equilibrium constant for eq 3 ( $K_3$ ) is not known (vide infra). Optical data suggest that  $K_3$  is small, since only very slight changes in the band at 512 nm were observed upon initial addition of  $\text{Bu}_4\text{N}^+\text{I}^-$ . It was not possible to obtain any quantitative data on the absorption spectrum of the ionic species. Optical data in support of dissociation were obtained for  $p\text{-CH}_3\text{-TPPFel}$  in acetone.<sup>34</sup> However, the complex is insufficiently soluble in this solvent to make NMR measurements practical.

In an effort to move the position of the equilibrium in eq 3 to the right and thereby speed up the inversion, we attempted to induce dissociation by "stripping" the iodide off of the complex.<sup>35</sup> A convenient reactant for this purpose was found to be  $\text{HgI}_2$ , which can tie up the free iodide ion via the reactions



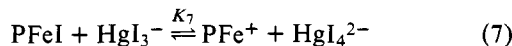
$K_4$  is quite large,<sup>36</sup> such that the dominant reaction could be written



Since  $\text{HgI}_2$  would increase dissociation to the ionic form of the porphyrin, the rate of inversion via dissociation should only increase with  $[\text{HgI}_2]$  over that of the pure complex. That the  $m\text{-H}$  peaks only increase in line width and collapse without first decreasing in width is illustrated in traces a, g-j in Figure 1. The effect of  $\text{HgI}_2$  on the rate of inversion ( $m\text{-H}$  collapse) is

also given in Figure 4. The contrast in the rate profile upon addition of  $\text{Bu}_4\text{N}^+\text{I}^-$ , an iodide donor (move eq 3 to the left), and  $\text{HgI}_2$ , an iodide acceptor (move eq 3 to the right), is abundantly clear in this figure.

Addition of  $\text{Bu}_4\text{N}^+\text{HgI}_3^-$  acts in a manner similar to  $\text{HgI}_2$ , only much less effectively. Hence  $\text{HgI}_3^-$  acts as an iodide acceptor, with the overall reaction



The fact that  $\text{HgI}_3^-$  acts as an iodide acceptor indicates that  $K_5$  is larger than  $K_3^{-1}$ . In the cases of the addition of either  $\text{HgI}_2$  and  $\text{HgI}_3^-$ , the collapsed *m*-H resonance could be resolved again simply by the addition of  $\text{Bu}_4\text{N}^+\text{I}^-$ .

In order to confirm the existence of the dissociative mechanism for the pure complexes,  $(\text{Bu}_4\text{N}^+)_2(\text{HgI}_4^{2-})$  was also added to *p*- $\text{CH}_3$ -TPPFeI. Here  $\text{HgI}_4^{2-}$  cannot act as an iodide acceptor, but can dissociate (eq 5) to provide  $\text{I}^-$ . In accordance with its only role as  $\text{I}^-$  donor, the rate of inversion first decreases, as depicted in Figure 4, and then increases again (as for  $\text{Bu}_4\text{N}^+\text{I}^-$ , only less effectively).

Optical data of chloroform solutions of  $\text{HgI}_2$  and *p*- $\text{CH}_3$ -TPPFeI support the iodide acceptor role of  $\text{HgI}_2$ . The electronic spectrum reveals that the band at 273 nm for  $\text{HgI}_2$  is shifted to 262 nm upon addition of *p*- $\text{CH}_3$ -TPPFeI, with an additional peak appearing at  $\sim 310$  nm. The new peaks correspond to  $\text{HgI}_3^-$ , for which bands at 261 and 306 nm have been reported.<sup>37</sup> In acetone, even the porphyrin peaks for the ionic form can be resolved.<sup>34</sup> Changes in the porphyrin band at  $\sim 500$  nm upon addition of  $\text{HgI}_2$  in chloroform were relatively minor, and attempts to resolve the components responsible for these changes were unsuccessful. However, addition of  $\text{Bu}_4\text{N}^+\text{I}^-$  to acetone and chloroform solutions qualitatively reversed the effect of  $\text{HgI}_2$ , and the spectra reverted to that of *p*- $\text{CH}_3$ -TPPFeI.

In no case was it possible to extract a rate law from the kinetic data involving dissociative inversion. This is due in part to the fact that the equilibrium constant  $K_3$  is unknown, and  $K_4$  and  $K_5$  are unavailable for  $\text{CDCl}_3$ . Furthermore, it was not possible to resolve any NMR signal attributable to the ionic form in any case, thus precluding a detailed kinetic analysis. The lack of resolution of the *m*-H signal (or *p*- $\text{CH}_3$ ) for the ionic species is probably due to the small concentration of these species and the fact that their NMR spectra likely resemble that of the parent neutral species. The proton shifts of high-spin *p*- $\text{CH}_3$ -TPPFeX complexes have been shown<sup>18,23</sup> to be relatively insensitive to X.

A number of reasonable reaction pathways which result in dissociative inversion for the pure complex are illustrated in Figure 5. Similar pathways can be postulated in the presence of  $\text{HgI}_2$ . The rates of porphyrin dissociation and recombination without inversion are  $k_1$  and  $k_{-1}$ , while the rate of dissociation and recombination with inversion are  $k_2$  and  $k_{-2}$ .  $k_0$  corresponds to inversion for the ionic complex; the activation enthalpy for this process would provide the elusive stabilization energy for the out-of-plane displacement for the iron atom. The case of inversion whereby a neutral complex is attacked by the free iodide resulting from dissociation of another molecule can be discarded, as evidenced by the effect of  $\text{Bu}_4\text{N}^+\text{I}^-$  on the rate of dissociative inversion. Another factor which may have to be considered is that some TPP-type complexes of high-spin iron tend to dimerize in solution, particularly those of weak axial ligands in  $\text{CD}_2\text{Cl}_2$  solution.<sup>32</sup> Thus, processes involving the reaction of  $\text{PFe}^+$  with PFeI to cause inversion may have to be considered in any detailed analysis.

#### Comments

The rates of porphyrin inversion via the associative mechanism reveal that this process is quite rapid, although the

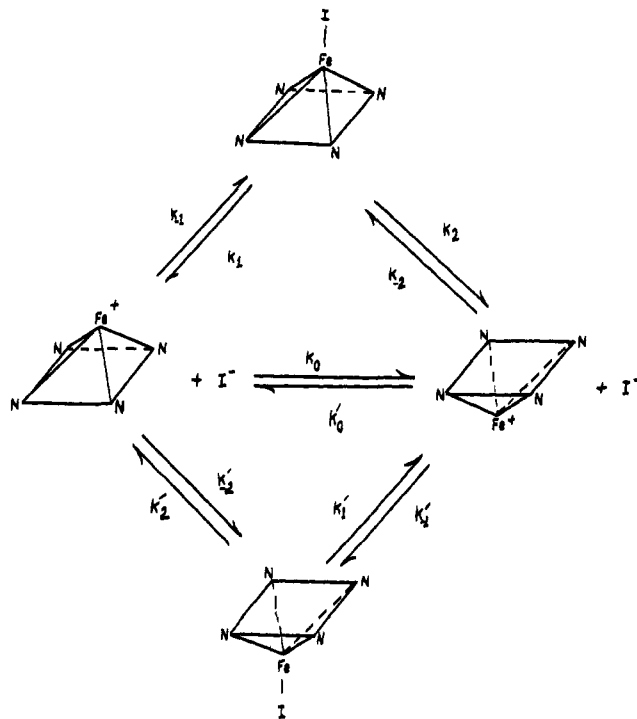


Figure 5. Possible dissociative pathways for iron "inversion" in iron porphyrins.

specific contribution to the activation enthalpy arising from the distortion necessary to fit the ferric ion into the hole could not be determined. The second-order rate constants, particularly in  $\text{CD}_2\text{Cl}_2$ , suggest a high degree of mobility for the iron relative to the heme plane. Similarly high inversion rates are indicated by the dissociative mechanism, although only quantitative rate data are available at this time.

Although a direct determination of the energy barrier for the movement of the unliganded ferric ion ( $k_0$  in Figure 5) into the porphyrin plane was not realized with the system investigated, some implications for the mobility of the ion can be drawn. The rate of *m*-H collapse (inversion) for TPPIInCl upon addition of  $\text{Bu}_4\text{N}^+\text{Cl}^-$  has recently been reported.<sup>38</sup> From the available data on *p*-*i*-Pr-TPPIInCl,<sup>31</sup> a second-order rate constant,  $k_2$  has been estimated at  $\sim 3 \times 10^4 \text{ M}^{-1} \text{ s}^{-1}$  in  $\text{C}_2\text{H}_2\text{Cl}_4$  at 30 °C. This value is similar to the  $k_2$  values for *p*- $\text{CH}_3$ -TPPFeCl/ $\text{Bu}_4\text{N}^+\text{Cl}^-$  system in  $\text{CD}_2\text{Cl}_2$  (see Table I). Since In(III) has a much larger ionic radius<sup>39</sup> (0.81 Å) than high-spin Fe(III) (0.53 Å), it appears unnecessary that the ferric ion revert to a low-spin form in order to pass through the porphyrin hole. In fact, In(III) is larger than high-spin Fe(II), suggesting that the biologically active ferrous ion can be expected to have similar mobility relative to the heme plane.<sup>6-9</sup>

Rather than focus on the energy required to fit the large, high-spin iron into the porphyrin plane in pseudoplanar porphyrins, it may be more realistic to inquire into the deformability of the porphyrin skeleton and the concomitant changes in the size of the hole. Extents of deviation from planarity in porphyrins and metalloporphyrins differ widely, from the planar  $\text{TPPSnCl}_2$ <sup>11</sup> to the highly ruffled diacids of tetrapyrrolylporphyrins.<sup>12</sup> This ruffling of the porphyrin skeleton causes substantial increases in the porphyrin hole as measured by the trans N-N distance. The optimal N-N distance of  $\sim 4.05 \pm 0.13$  Å in planar systems<sup>2,10</sup> is increased to  $\sim 4.28$  Å in the distorted diacid.<sup>12</sup> Such large distortions could easily accommodate the high-spin ions within the hole. The high degree of mobility of the iron relative to the heme plane, therefore, suggests that porphyrins do undergo high-amplitude vibrations

resembling the ruffling of the skeleton as a mechanism for effecting inversion of five-coordinate porphyrins with sizable out-of-plane displacements, as characterized in static structures.

The rate constants in Table I and the kinetic parameters in Table II represent inversion as induced by associative halide exchange occurring exclusively via an SN2 mechanism. Any halide exchange occurring on the same side of the porphyrin goes undetected in the NMR method<sup>15</sup> employed here. Thus the present system represents one of the most thoroughly characterized cases of axial ligand lability in metalloporphyrins.<sup>19</sup>

**Acknowledgment.** The authors are indebted to Professor F. Basolo for a stimulating discussion, to Professor Innhofen for a gift of OEP, and to the National Institute of Health (HL-16087) for support of this research.

## References and Notes

- (1) Fellow of the Alfred P. Sloan Foundation.
- (2) (a) J. L. Hoard, *Science*, **174**, 1295 (1971); (b) J. L. Hoard, M. J. Hamor, T. A. Hamor, and W. S. Caughey, *J. Am. Chem. Soc.*, **87**, 2312 (1965); D. F. Koenig, *Acta Crystallogr.*, **18**, 663 (1965).
- (3) J. L. Hoard, C. H. Cohen, and M. D. Glick, *J. Am. Chem. Soc.*, **89**, 1992 (1967).
- (4) D. M. Collins, R. Countryman, and J. L. Hoard, *J. Am. Chem. Soc.*, **94**, 2066 (1972).
- (5) L. J. Rabinovich, A. Bloom, and J. L. Hoard, *J. Am. Chem. Soc.*, **94**, 2073 (1972).
- (6) M. F. Perutz, *Nature (London)*, **228**, 726 (1970).
- (7) J. C. Kendrew, *Science*, **139**, 1259 (1963); R. Huber, O. Epp, and H. Formanek, *J. Mol. Biol.*, **42**, 591 (1971).
- (8) M. F. Perutz and L. F. TenEyck, *Cold Spring Harbor Symp. Quant. Biol.*, **36**, 295 (1971); M. F. Perutz, *Nature (London)*, **237**, 495 (1972).
- (9) R. J. P. Williams, *Cold Spring Harbor Symp. Quant. Biol.*, **36**, 53 (1971).
- (10) E. B. Fleischer, *Acc. Chem. Res.*, **3**, 105 (1970).
- (11) D. M. Collins, W. R. Sheidt, and J. L. Hoard, *J. Am. Chem. Soc.*, **94**, 6689 (1972).
- (12) A. L. Stone and E. B. Fleischer, *J. Am. Chem. Soc.*, **90**, 2735 (1968).
- (13) T. A. Hamor, W. S. Caughey, and J. L. Hoard, *J. Am. Chem. Soc.*, **87**, 2305 (1965).
- (14) M. Zerner, M. Gouterman, and H. Kobayashi, *Theor. Chim. Acta*, **6**, 363 (1966).
- (15) G. N. La Mar, *J. Am. Chem. Soc.*, **95**, 1662 (1973).
- (16) G. N. La Mar, *Pure Appl. Chem.*, **40**, 13 (1974).
- (17) G. N. La Mar, G. R. Eaton, R. H. Holm, and F. A. Walker, *J. Am. Chem. Soc.*, **95**, 63 (1973).
- (18) F. A. Walker and G. N. La Mar, *Ann. N.Y. Acad. Sci.*, **206**, 328 (1973).
- (19) G. N. La Mar and F. A. Walker, *J. Am. Chem. Soc.*, **94**, 8607 (1972).
- (20) E. B. Fleischer, S. Jacobs, and L. Mestichelli, *J. Am. Chem. Soc.*, **90**, 2527 (1968); G. B. Kolski and R. A. Plane, *ibid.*, **94**, 3740 (1972); B. B. Hasinoff, H. B. Dunford, and D. G. Horne, *Can. J. Chem.*, **47**, 3225 (1969); N. S. Angerman, B. B. Hasinoff, H. B. Dunford, and R. B. Jordan, *ibid.*, **47**, 3217 (1969); J. Hodgkinson and R. B. Jordan, *J. Am. Chem. Soc.*, **95**, 763 (1973); H. A. Degani and D. Fiat, *ibid.*, **93**, 4281 (1971).
- (21) C. G. Grimes and R. G. Pearson, *Inorg. Chem.*, **13**, 970 (1974); C. G. Grimes, Ph.D. Thesis, Northwestern University, 1973.
- (22) A. D. Adler, F. R. Longo, F. Kampas, and J. Kim, *J. Inorg. Nucl. Chem.*, **32**, 2443 (1970).
- (23) G. N. La Mar and F. A. Walker, *J. Am. Chem. Soc.*, **95**, 6950 (1973).
- (24) M. F. Reich and I. A. Cohen, *J. Inorg. Nucl. Chem.*, **32**, 343 (1970).
- (25) C. R. Witschanke and C. A. Kraus, *J. Am. Chem. Soc.*, **69**, 2473 (1947).
- (26) This program was kindly provided by L. H. Pignolet.
- (27) J. A. Pople, W. G. Schneider, and H. J. Bernstein, "High Resolution Nuclear Magnetic Resonance", McGraw-Hill, New York, N.Y., 1959, Chapter 10.
- (28) G. N. La Mar and E. O. Sherman, *J. Am. Chem. Soc.*, **92**, 2691 (1970).
- (29) M. Mometeau, J. Mispelter, and D. Lexa, *Biochim. Biophys. Acta*, **322**, 38 (1973).
- (30) J. T. Thomas and D. F. Evans, *J. Phys. Chem.*, **74**, 3812 (1970); M. A. Matesich, J. A. Nadas, and D. F. Evans, *ibid.*, **74**, 4568 (1970); D. F. Evans, J. Thomas, J. A. Nadas, and M. A. Matesich, *ibid.*, **75**, 1714 (1971).
- (31) The large uncertainty in  $\Delta H^\ddagger$  for inversion in the case of *p*-CH<sub>3</sub>-TPPFeCl is due to the fact that at the temperatures where inversion kinetics were determined, the two *m*-H protons can also average by phenyl rotation (G. R. Eaton and S. S. Eaton, *J. Am. Chem. Soc.*, **97**, 3660 (1975)). This process is concentration independent so that it can be clearly distinguished from inversion. The two processes overlap in the temperature range 20–30 °C. Although attempts were made to correct for phenyl rotation kinetics, the inability to clearly define the phenyl rotation kinetic parameter introduces sizable uncertainties in the line broadening due to inversion.
- (32) There is some evidence that these porphyrin dimerize in CD<sub>2</sub>Cl<sub>2</sub> (R. V. Snyder and G. N. La Mar, unpublished observations). Thus the molecularity of the associative invasion with respect to Bu<sub>4</sub>N<sup>+</sup>X<sup>-</sup> is 1.0, but only ~0.9 with respect to porphyrin. This small extent of dimerization at 25°, however, is unlikely to affect the relative rates of inversion for different parasubstituents.
- (33) J. E. Falk and J. N. Phillips, *Nature (London)*, **212**, 153 (1966); W. S. Caughey, W. Y. Fujimoto, and B. P. Johnson, *Biochemistry*, **5**, 3830 (1966).
- (34) In acetone, addition of HgI<sub>2</sub> to *p*-CH<sub>3</sub>-TPPFeI caused a decrease in the 512-nm band and the growth of a new peak at 527 nm. Subsequent addition of Bu<sub>4</sub>N<sup>+</sup>I<sup>-</sup> reversed the process.
- (35) The authors are indebted to F. Basolo for this suggestion.
- (36) F. Gaizer and G. Johansson, *Acta Chem. Scand.*, **22**, 3013 (1968); M. A. Hooper and D. W. James, *Aust. J. Chem.*, **24**, 1345 (1971).
- (37) G. B. Deacon, *Rev. Pure Appl. Chem.*, **13**, 189 (1963).
- (38) S. S. Eaton and G. R. Eaton, *J. Chem. Soc., Chem. Commun.*, 576 (1974).
- (39) F. A. Cotton and G. Wilkinson, "Advanced Inorganic Chemistry", Interscience, New York, N.Y., 1966.

## Solute Complexes in Aqueous Gadolinium(III) Chloride Solutions

Marcus L. Steele and D. L. Wertz\*

Contribution from the Department of Chemistry, University of Southern Mississippi, Hattiesburg, Mississippi 39401. Received September 16, 1975

**Abstract:** The structure of the average solute species in two concentrated aqueous solutions of GdCl<sub>3</sub>, with and without added hydrochloric acid, has been measured. In each solution Gd<sup>3+</sup> has 8 (±0.2) nearest neighbors. The average solute species are Gd(H<sub>2</sub>O)<sub>8</sub><sup>3+</sup> in the aqueous solution and Cl<sub>2</sub>Gd(H<sub>2</sub>O)<sub>6</sub><sup>+</sup> in the solution in which hydrochloric acid is the solvent. The average Gd–O nearest neighbor distance has been measured to be 2.37 (±0.02) Å, and the nearest neighbor Gd–Cl distance has been calculated to be ca. 2.8 Å. The ion-pair Gd···Cl distance ranges from 4.8 to 5.0 Å. On the average, dichlorohexaquo-gadolinium(III) appears to be pseudocubic (*D*<sub>3h</sub>), but no satisfactory solute model of Gd(H<sub>2</sub>O)<sub>8</sub><sup>3+</sup> has been found.

## Introduction

Interest in the aqueous solution chemistry of Gd<sup>3+</sup> has dramatically increased in the past few years because of its frequent use as a lanthanide shift reagent,<sup>1</sup> a probe in studying metal-amino acid complexes,<sup>2,3</sup> and because of the "gadolinium break"<sup>4</sup> observed in many thermodynamic measurements of solutions containing various lanthanide salts. Notwithstanding, the solution chemistry of Gd<sup>3+</sup> has not been thoroughly studied and is not well understood. As noted by Mioduski and Siekierski,<sup>5</sup> considerable question still exists regarding the coordination number(s) of the various lan-

thanide break<sup>4</sup> observed in many thermodynamic measurements of solutions containing various lanthanide salts. Notwithstanding, the solution chemistry of Gd<sup>3+</sup> has not been thoroughly studied and is not well understood. As noted by Mioduski and Siekierski,<sup>5</sup> considerable question still exists regarding the coordination number(s) of the various lan-